analytical chemistry

Article

pubs.acs.org/ac

# Copper-Based Electrochemical Sensor with Palladium Electrode for Cathodic Stripping Voltammetry of Manganese

Wenjing Kang,[†] Xing Pei,[†] Adam Bange,[‡] Erin N. Haynes,[§] William R. Heineman,[∥] and Ian Papautsky*[,†]

[†]BioMicroSystems Lab, Department of Electrical Engineering and Computing Systems, University of Cincinnati, Cincinnati, Ohio 45221-0030, United States

[‡]Department of Chemistry, Xavier University, Cincinnati, Ohio 45207-4221, United States

[§]Department of Environmental Health, University of Cincinnati, Cincinnati, Ohio 45267-0056, United States

[∥]Department of Chemistry, University of Cincinnati, Cincinnati, Ohio 45221-0172, United States

Supporting Information

**ABSTRACT:** In this work, we report on the development of a palladium-based, microfabricated point-of-care electrochemical sensor for the determination of manganese using square wave cathodic stripping voltammetry. Heavy metals require careful monitoring, yet current methods are too complex for a point-of-care system. Voltammetry offers an attractive approach to metal detection on the microscale, but traditional carbon, gold, or platinum electrodes are difficult or expensive to microfabricate, preventing widespread use. Our sensor uses palladium working and auxiliary electrodes and integrates them with a copper-based reference electrode for simple fabrication and compatibility with microfabrication and printed circuit board processing, while maintaining competitive performance in electrochemical detection. Copper electrodes were prepared on glass substrate using a combination of microfabrication procedures followed by electrodeposition of palladium. The disposable sensor system was formed by bonding a poly(dimethylsiloxane) (PDMS) well to the glass substrate. Cathodic stripping voltammetry of manganese using our new disposable palladium-based sensors exhibited 334 nM (18.3 ppb) limit of detection in borate buffer. The sensor was used to demonstrate manganese determination in natural water samples from a pond in Burnet Woods, located in Cincinnati, OH, and the Ohio River.

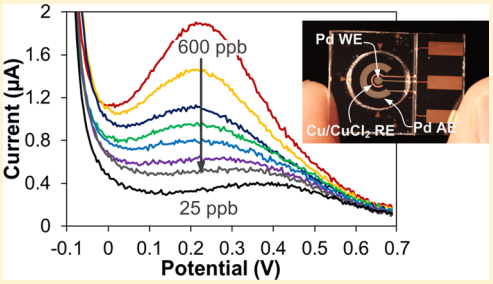


Monitoring manganese (Mn) in the environment has become increasingly important because of greater use in various products and better understanding of its adverse effects on health. Mn is an essential element that is critical to metabolism due to its involvement in enzyme activation; yet, it is toxic in high concentrations[1,2] and has been associated with development of Parkinson's disease[3−5] and impaired neurological function in children.[6,7] Natural water, the atmosphere, and soil are all sources of Mn exposure, which vary widely in concentration. The most commonly acknowledged anthropogenic sources of Mn include mining, production and refining of Mn alloys, and steel production.[8−10] Apart from industry, agricultural cultivation, fertilizer, and use of fungicides, such as maneb and mancozeb,[11] are also potential sources for human exposure. Other concerns include the manganese-based additive methylcyclopentadienyl manganese tricarbonyl (MMT)[12,13] that replaced lead (Pb) in gasoline as an antiknock agent, and Mn use in rechargeable cell phone batteries.[14] According to the toxicological profile for Mn issued by the Agency for Toxic Substances and Disease Registry, the highest acceptable level of Mn is only 50 ppb (0.91 μM)[15] for drinking water. A recent case reported elevated biological concentration of Mn in blood, hair, and urine of a 10 year old child; the only identified source was from the residence's well water (1.21 ppm).[16] Thus, there is a growing need for analytical methods that can be used to precisely monitor the concentration of Mn at low levels in a variety of media from drinking water to bodily fluids in humans.

The conventional methods for determining Mn are based on atomic absorption spectroscopy (AAS) or inductively coupled plasma mass spectrometry (ICPMS). These methods provide high accuracy and sensitivity, but suffer from a number of disadvantages. The bulky instrument, severe delays in turn-around time due to shipping to a centralized lab, requirement for specialized personnel, and expensive cost all prevent these techniques from being applied in point-of-care (POC) measurements. Electrochemical techniques, such as stripping voltammetry,[17,18] offer a viable option with more rapid analysis, simpler instrumentation, and lower cost, which is more suitable for POC applications. And, it is capable of limits of detection (LODs) in the sub-part-per-billion (μg/L) range. Stripping voltammetry involves a preconcentration step during which the working electrode is biased at a certain potential until an adequate amount of target analyte has been deposited at the electrode and a stripping step to remove the deposited analyte

**Received:** July 27, 2014
**Accepted:** November 18, 2014
**Published:** December 5, 2014

  

from the electrode surface while generating a faradaic current that is related to the analyte concentration in the sample.

Anodic stripping voltammetry (ASV) has been considered as the most widespread, trace-level electrochemical sensing technique,[19] which defines the preconcentration step to happen at a potential to reduce target analyte, and the stripping step scanning in the positive direction to strip the deposited analyte by oxidation giving anodic current that is measured for quantification. However, ASV is challenging for Mn determination because the very negative potential needed to reduce Mn ions does not fit the negative potential working ranges of most solid electrodes. Previous measurements of Mn using Bi or carbon nanotube (CNT) electrodes[4,5,20] produced distorted voltammograms and obscure peaks because the Mn stripping peak occurs at a very negative potential which is close to the reduction potential of $H^+$. Thus, an alternative approach to circumvent the interference from $H^+$ reduction current is needed for reliable and accurate determination of Mn at the low concentrations required for practical applications.

Cathodic stripping voltammetry (CSV) is an alternative approach to ASV that offers a number of advantages for determining Mn. CSV is the electrochemical reverse of ASV and is performed by preconcentrating at a potential to oxidize aqueous ions to insoluble oxides that deposit on the electrode, followed by stripping in the negative potential direction to reduce them back to the soluble ionic form giving cathodic current that is measured for quantification. Figure 1a illustrates

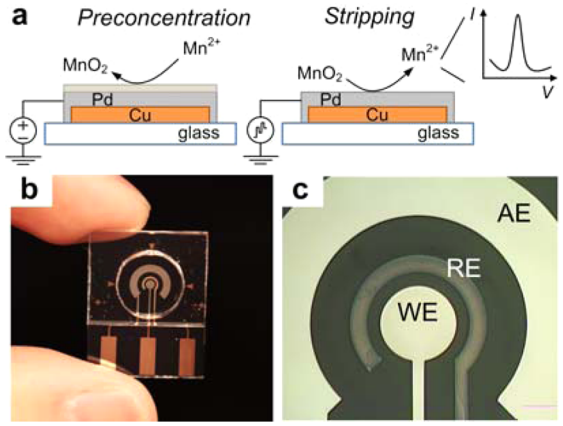


**Figure 1.** (a) Schematic diagram of CSV of Mn on an electroplated Pd electrode showing the preconcentration step to oxidize Mn(II) into Mn(IV) which forms a layer of $MnO_2$ on the surface of the Pd WE, and the stripping step to reduce Mn(IV) back to Mn(II) off from the electrode. (b) Photograph of the sensor. (c) A close-up of the electrodes: Pd WE and AE, Cu/$CuCl_2$ RE (WE = working electrode, RE = reference electrode, AE = auxiliary electrode).

the key steps for CSV of Mn, with trace Mn(II) being oxidized to Mn(IV) which hydrolyzes into insoluble manganese dioxide or hydrate on the electrode surface. Compared with ASV, the CSV approach is less susceptible to oxygen and intermetallic interferences. Also, a large selection of common electrode materials is available for CSV. Apart from mercury,[21] which is toxic and not environmentally friendly, this approach has been used with platinum,[22−25] glassy carbon or carbon film,[26−28] graphite,[29] CNT,[5,30] or boron-doped diamond electrodes.[4,31] Despite the stable performance and low detection limits on some of these materials, miniaturization and integration of such electrodes into POC sensor systems remain challenging.

Herein, we discuss the use of the copper (Cu)-based sensor we reported recently[32] for determination of Mn by CSV. The copper-based sensor presents a good platform for POC determination of metals, with demonstrated excellent performance for ASV determination of zinc and lead. However, the Cu working electrode (WE) is not suitable for Mn determination by either form of stripping voltammetry due to insufficient potential range. It lacks the negative potential range needed for ASV of Mn, and it is not suitable for CSV of Mn either because its oxidation at positive potentials prevents formation of Mn(IV) in the deposition step. Thus, to broaden the potential window and protect electrodes from degradation by oxidation, we electrodeposited a thin layer of palladium (Pd) on both the Cu WE and the Cu auxiliary electrode (AE) as shown in the close-up photograph of the sensor electrodes in Figure 1c. However, to simplify fabrication, we continue to use the Cu/$CuCl_2$ reference electrode (RE), which we previously showed to offer sufficiently stable performance in anodic stripping for disposable sensors. The Pd WE sensor exhibits favorable response for Mn in pH 9.0, 0.1 M borate buffer with a detection limit of 334 nM (18.3 ppb). Using the sensor in a standard addition approach, we successfully measured 1.74 $\mu$M (95.5 ppb) Mn in sample of water from the Ohio River. This work showcases the flexibility of the copper-based sensor design, which can be easily modified by simple coating of the working electrode. This is also the first demonstration of Mn determination by CSV on a microscale sensor. Ultimately, with additional integration of miniaturized potentiostat electronics, a portable sensor system capable of Mn determination in water samples is envisioned.

## EXPERIMENTAL SECTION

**Reagents.** Reagents were prepared from chemicals purchased from Thermo Fisher Scientific, unless noted otherwise. Piranha solution was prepared from $H_2SO_4$ and $H_2O_2$ in 7:3 (v/v) ratio. Copper etchant was prepared from $H_2O_2$, $H_2SO_4$, and deionized (DI) water in 1:1:10 (v/v/v) ratio. Titanium etchant was prepared from $HNO_3$, HF, and DI water in 1:2:7 (v/v/v) ratio. Palladium electroplating solution was purchased from Technic Inc. (PALLASPEED RTU). A 1 M borate buffer was purchased from Sigma-Aldrich. A 0.1 M borate buffer was prepared by dilution of the commercial buffer with DI water. Borate buffers with pH from 8.0 to 9.75 were prepared by addition of NaOH(s) to the diluted commercial buffer. Solutions containing 25−600 ppb (455 nM to 10.9 $\mu$M) Mn were prepared by diluting Mn stock solution (TraceCERT, 1000 mg/L $Mn^{2+}$ in 2% nitric acid, Fluka Analytical) with borate buffer.

**Sensor Fabrication.** The fabrication procedures for the palladium-coated Cu electrochemical sensor include a single photolithography step, followed by two electrodeposition steps. Metal layers of 20 nm of titanium (Ti)/200 nm Cu were then evaporated (Temescal FC-1800 E-Beam evaporator) onto glass substrates cleaned in Piranha solution. An etch mask of ∼2 $\mu$m was formed using photolithography with Shipley 1818 photoresist and developer 351. The three-electrode patterns with contact pads were formed by wet etching in Cu etchant for 10 s followed by Ti etchant for 3 s, with 1 min of rinse in DI water after each etching step. A polymer well with ∼9 mm diameter and 3 mm thickness was fabricated in poly(dimethylsiloxane) (PDMS) using the standard soft lithography process. It was bonded to a clean glass substrate containing the electrode patterns using plasma discharge (BD-20AC, Electo-


dx.doi.org/10.1021/ac502882s | Anal. Chem. 2014, 86, 12070−12077

Technic Products Inc.) after 20 s of treatment on the PDMS surface only. An interface consisting of an edge-board connector (EBC05DRAS, Sullins) and a mini-USB port were soldered on a printed circuit board to simplify and improve connection between the sensor and the potentiostat. The surface area for the WE, RE, and AE are 0.019, 0.023, and 0.139 $cm^2$, respectively. The Pd WE and AE were formed by deposition of Pd at 5 $mA/cm^2$ cathodic current for 90 s with a Pt wire AE to sustain the current. The $Cu/CuCl_2$ RE was fabricated by chloridizing Cu in 1 M KCl with a 3 $mA/cm^2$ anodic current for 30 s.

**Samples.** We chose two natural water samples to analyze using our sensor. The pond water sample was collected from Burnet Woods pond (Cincinnati, OH, August 9, 2013). River water sample was collected from the Ohio River (Newport, KY shore, November 30, 2012). Both samples were collected in conical tubes (Falcon 15 mL conical centrifuge tubes), at least 10 mL volume. Samples were diluted with 0.2 M borate buffer (pH 9.0) by a factor of 2, which yielded pH 8.96. Samples were analyzed immediately upon completion of dilution using the method of standard additions discussed below.

**Electrochemical Experiments.** A miniature USB potentiostat (WaveNow, Pine Instruments, Inc.) with AfterMath Data Organizer software was used for all electrochemical measurements. A sensor was inserted into the interface and connected to the potentiostat using a mini-USB cable. The sample volume was 100 $\mu$L for all the experiments in borate buffer. For the study of stability of our $Cu/CuCl_2$ RE, we measured open circuit potential (OCP) between the $Cu/CuCl_2$ RE and a double-junction Ag/AgCl RE (MI-401F, Microelectrodes Inc.), which was used as a standard reference electrode. We performed cyclic voltammetry (CV) in pH 9.0 0.1 M borate buffer to confirm the potential window of the electrodeposited Pd electrode and the position of the Mn reduction peak. After a series of optimizations of CSV parameters in pH 9.0, 0.1 M borate buffer, we used the following parameters: 0.7 V as preconcentration potential with 600 s duration, stripping range from 0.7 to −0.2 V; waveform parameters of 70 ms for period, 4 mV for increment, and 25 mV for amplitude. Manganese from 455 nM (25 ppb) to 10.9 $\mu$M (600 ppb) in borate buffer was used to construct the calibration curve and calculate LOD as $3\sigma$/slope. We used the same stripping parameters for the detection of Mn concentrations in natural water samples, while using the method of standard addition to determine the concentration of Mn in the original samples.

## RESULTS AND DISCUSSION

**Novel Pd WE Sensor.** Our previous work[20,33] demonstrated a miniature electrochemical sensor with a Bi WE for determination of Mn, which exhibits a very negative stripping potential. The sensor was approximately 15 × 19 $mm^2$, required only microliters of sample, and performed an analysis in less than 15 min. Although the Bi WE performed reasonably well, with LOD = 5 $\mu$M, the shape of the stripping peak was not ideal and it occurred on the shoulder of $H^+$ reduction current despite optimization efforts. In addition, the fabrication procedure for these electrodes was complex and costly, requiring multiple photolithography, e-beam evaporation, and lift-off process steps.

To address the aforementioned shortcomings of the Bi WE sensors, we developed a sensor for cathodic stripping of Mn based on a Pd thin film. We used Pd due to its similarity with Pt and the ability to offer stable performance at the positive potential used for the preconcentration step in CSV of Mn.[34−38] Pt offers stable performance, but the high cost and difficulties in fabrication make it less desirable for disposable devices. The commonly used Au exhibits a reduction peak that overlaps with the cathodic stripping peak of Mn. Ultimately, Pd offers a sufficiently wide potential window for CSV of Mn, and at a substantially lower cost.

Fabrication of our new Pd WE sensor is based on the Cu thin-film electrochemical cell we introduced recently specifically for POC applications.[32] Our sensor consists of a Pd WE, a Pd AE, and a $Cu/CuCl_2$ RE, as illustrated in Figure 1b. To simplify fabrication, the Pd layer for the WE and AE was electrodeposited on top of a patterned Cu seed layer. In prior work we used this Cu seed layer for direct determination of metals with mildly negative stripping potentials, such as Zn.[32] Here, however, the Cu WE proved to be inadequate for determining Mn as its potential window was simply not sufficiently negative to permit anodic stripping of Mn or sufficiently positive for cathodic stripping of Mn. For the RE, using $Cu/CuCl_2$ can further simplify fabrication and eliminate the additional step of electroplating silver in the fabrication of a Ag/AgCl RE. The layout of the electrode patterns was generally similar to our earlier work, with a user-friendly interface that integrated an edge-board connector and a mini-USB port to provide simplified connection and accessibility.

**Pd Auxiliary Electrode.** Since the AE in an electrochemical cell must provide stable current during both preconcentration and stripping steps, we first assessed stability of the Pd AE. In conventional electrochemical cells, AEs are fabricated from inert materials, such as Pt or graphite. Since Pd is a platinum group metal, we expected it to perform similarly to Pt. We compared these two metals using chronopotentiometry at 10 $\mu$A current, which is the typical upper limit of current we see in cathodic stripping experiments. During this experiment, we used a graphite electrode as the cathode, with Pd or Pt as the anode. As expected, the Pt electrode maintained a stable potential at about 1.3 V for the oxidation of water during the entire 60 min experiment (Figure 2a), indicating that it is an

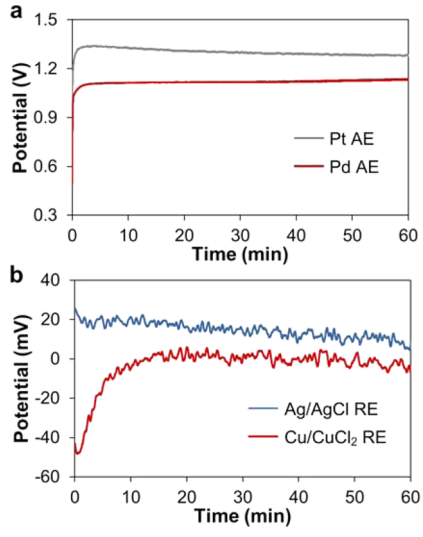


**Figure 2.** (a) Comparison of the electroplated Pd AE vs a Pt wire AE in pH 9.0 borate buffer. (b) Comparison of the response time and stability of the integrated $Cu/CuCl_2$ RE vs Ag/AgCl RE in pH 9.0 borate buffer.


dx.doi.org/10.1021/ac502882s | Anal. Chem. 2014, 86, 12070−12077

excellent, perfectly polarizable AE. The electrodeposited Pd AE was also perfectly polarizable and sustained a potential of approximately 1.1 V. This experiment showed that a thin layer of Pd film could protect the Cu layer underneath from oxidation and ensure reproducibility of measurements with even long preconcentration times. Next, we examined the electrochemical performance of the $Cu/CuCl_2$ RE.

**$Cu/CuCl_2$ Reference Electrode.** Although we demonstrated stability of the microfabricated $Cu/CuCl_2$ RE in acidic buffer in our previous work,[32] herein we investigated its stability under the basic buffer conditions necessary for CSV of Mn by comparing it with the commonly used Ag/AgCl RE. Excessive instability of the reference electrode can lead to difficulties in peak assignment in samples that contain mixtures of metals and give multiple peaks, or can interfere with peak quantitation if an incorrect deposition potential is applied. By monitoring the OCP against a commercially available double-junction Ag/AgCl RE in pH 9.0, 0.1 M borate buffer, we observed differences between the two REs (Figure 2b). For the $Cu/CuCl_2$ RE, this difference compared to the commercial RE reached a stable value of 3.4 ± 9.8 mV in 306 s, while for the Ag/AgCl RE the difference was approximately 14.6 ± 3.9 mV in 68 s. This difference in the response time may be due to differences in solubility of $CuCl_2$ and AgCl in pH 9.0 borate buffer.

Our previous results[32] show the response times of the two REs in acetate buffer to be 28 and 46 s, respectively, which suggests that, in basic buffer, it takes longer for some of the chloride layer of the REs to dissolve and stabilize the RE. To further confirm the response time of $Cu/CuCl_2$ RE, we evaluated the potential between WE and RE during the preconcentration step of CSV using a potentiostat and an independent multimeter and found that the potential reached the designated value within 8 s. The drift in the reference electrode potential can cause quantitative and qualitative errors in data collection and analysis beyond simple inaccuracies in the measured potential. After ~10 min, when the potentials of both REs equilibrated, we calculated the drift rate of our electrodes. The $Cu/CuCl_2$ RE drifted at a rate of ~1.5 mV/h, while the Ag/AgCl RE drifted at ~15.2 mV/h. These rates are higher than that of some microscale Ag/AgCl REs reported in literature[39,40] that exhibit drift of ~0.034 mV/h, but are lower than our previous measurements of $Cu/CuCl_2$ RE in saturated KCl solution (4.6 M at 20 °C) that showed a drift rate of ~0.3 mV/min.[32] Nevertheless, the drift rate of the $Cu/CuCl_2$ RE in borate buffer is quite low, and we believe it would be able to provide a stable potential during the stripping step if the preconcentration time is shorter than 10 min. The more convenient fabrication process combined with its acceptable stability in buffer makes the integrated $Cu/CuCl_2$ RE an attractive option for this sensor compared to the conventional Ag/AgCl reference electrode. Having established that Pd AE and copper-based RE are possible, we focused on determining if Pd can be used as a working electrode for Mn CSV.

**Pd Working Electrode.** As the first step in evaluating the Pd WE, we performed CV to evaluate the potential window of the Pd WE and the potential of the reduction peak of manganese oxide by scanning from −1 to 0.8 V at the rate of 100 mV/s in 0.1 M borate buffer with different pHs. The voltammograms were carefully examined and compared (see the Supporting Information). On the basis of these comparisons, pH 9.0 was selected because the $Mn^{2+}$ ion is not sufficiently soluble in more basic pHs. At this pH, a flat region from 700 mV to ~0 V can be clearly observed, which indicates the potential range suitable for reduction of metals.

Adding 10 ppm Mn to the buffer illustrates the reduction peaks for Mn in the 0 to 200 mV range (Figure 3b). The Pd

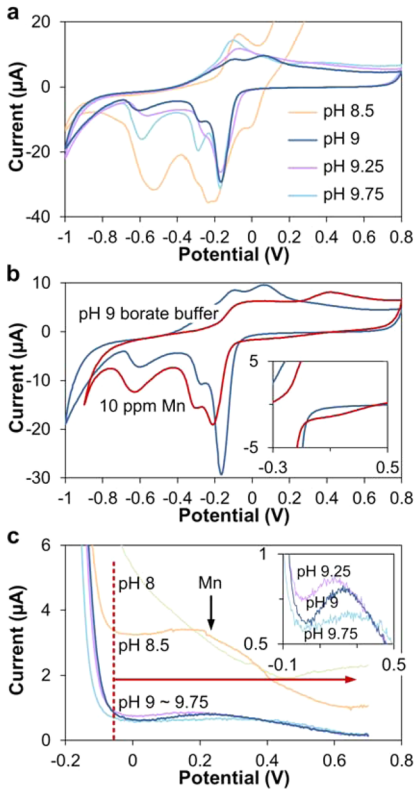


**Figure 3.** (a) CVs of electroplated Pd WE in 0.1 M borate buffer of various pH. (b) CV of pH 9, 0.1 M borate buffer alone and with additional 10 ppm Mn; the inset illustrates close-up of the Mn reduction peak. (c) CSV of 5 μM Mn at different pHs of borate buffer, with the inset illustrating the Mn stripping peak. The red arrow marks the potential range for this Pd electrode.

reduction peaks in both curves correspond to reduction of a thin layer of palladium oxide covering the surface of the Pd WE.[41] Considering that the peaks occurred far more negative than Mn reduction, at −170, −270, and −600 mV for borate buffer, and −200, −300, and −630 mV for buffer with 10 ppm Mn, we believe they would not interfere with the stripping process of manganese oxide in CSV. The potential range of the Pd WE in different pHs was further demonstrated by CSV of 5 μM Mn (Figure 3c).

We optimized the current density used for electrodeposition of the Pd film on WE and AE before optimizing parameters for stripping voltammetry. On the basis of the earlier work on electrodeposition of Pd[42,43] and the information provided by the manufacturer of the plating solution, we defined the range of deposition current from 700 μA to 1 mA (~4.4−6.3 mA/$cm^2$, since the total surface area of WE + AE = 0.158 $cm^2$). Four values of plating current were evaluated (Figure 4a) according to the film thickness, surface morphologies, and most importantly, peak shape and amplitude of the Mn stripping voltammograms, by performing CSV in a 100 μL sample with 5 μM Mn. The average thickness of the Pd film was ~100 ± 10 nm for all four currents, while the surface roughness varied according to plating current.


dx.doi.org/10.1021/ac502882s | Anal. Chem. 2014, 86, 12070−12077

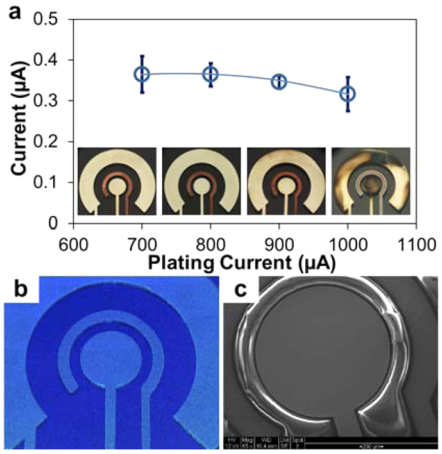


**Figure 4.** Optimization of plating current for electrodeposition of Pd: (a) CSV peak current (ordinate) of 5 $\mu$M Mn with electrode deposited by four plating currents (abscissa), while the inset illustrates their surface condition. (b) Optical profiler scans and (c) SEM of Pd electrode deposited with 800 $\mu$A current.

Although 1 mA current generated a slightly thicker film, hydrogen embrittlement occurred causing higher surface roughness of ~8.0 ± 4.2 nm and a burned appearance on the film.[42,44] Also, the film exhibited stress that led to curled edges that tended to peel off even with delicate handling. Thus, the Mn stripping signal was small and had a large variation (Figure 4a). The Pd film generated by 900 $\mu$A current suffered from the same issue as 1 mA, only to a smaller extent with a roughness of 2.3 ± 1.4 nm. The film quality improved as the current decreased to 800 $\mu$A, which no longer showed burned spots and the surface roughness was reduced to 1.4 ± 0.8 nm. The current of 700 $\mu$A seemed not enough since the film roughness increased to 4.0 ± 2.2 nm, and a faint pink color suggested only partial coverage of the Cu substrate. While the Mn peak from electrodes plated by 700 $\mu$A current provided acceptable amplitude, the variability was not favorable. The results from Mn stripping and their reproducibility in Figure 4a illustrate 800 $\mu$A (~5.1 mA/cm$^2$) to be the optimal value of current, based on the largest signal amplitude and small variation. Figure 4, parts b and c, shows a smooth Pd film on electrodes deposited by 800 $\mu$A current. With the deposition parameter finalized, we examined the buffer condition for preconcentration of Mn.

**Optimization of CSV Parameters.** To further explore the electrochemical characteristics of the Pd WE sensor, we investigated the effect of buffer pH on the stripping of Mn. CSV was performed in 0.1 M borate buffers with pHs in the 8–9.75 range. As results in Figure 5a demonstrate, for pH = 8 buffer no detectable Mn was observed because the solution was too acidic for manganese oxide to form or remain stable. Although it was possible to measure Mn at pH 8.5, the voltammograms suffered from substantial signal noise, which led to significant variability. More basic pH ≥ 9 provided a suitable environment for the formation of $MnO_2$, but no distinct differences could be observed from the voltammograms. Since $Mn^{2+}$ precipitates easily in buffer pH > 10, we chose pH 9.0 which gave the largest peak amplitude and best reproducibility.

The preconcentration step is critical in any stripping technique, and thus we optimized this step for CSV. The preconcentration potential was varied from 0.6 to 0.9 V with

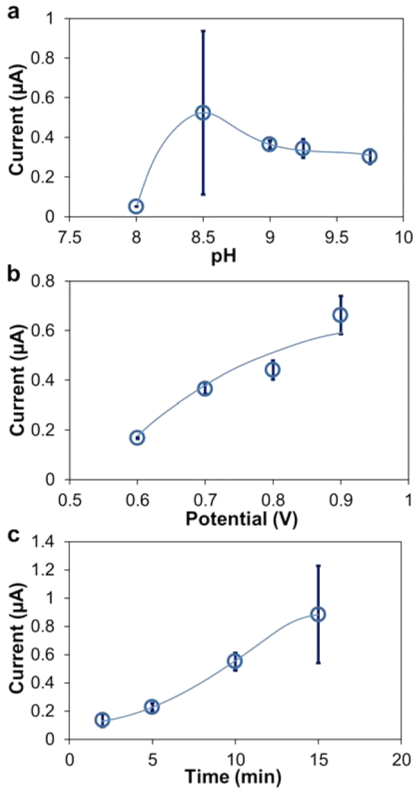


**Figure 5.** Optimization of parameters for CSV of Mn by comparisons of the amplitude and reproducibility of the Mn cathodic stripping peak in 5 $\mu$M Mn in pH 9.0, 0.1 M borate buffer solution: (a) pH of borate buffer; (b) preconcentration potential; (c) preconcentration time.

intervals of 0.1 V. As results in Figure 5b show a potential of 0.6 V was too negative to maximize oxidation of $Mn^{2+}$; thus, the amplitude of the manganese oxide reduction peak was rather small. The peak amplitude was improved at potentials more positive than 0.6 V, but Pd oxidation became predominant above 0.8 V, and the peak we observed on the voltammograms shifted from ~300 to 650 mV, due to reduction of a largely increased amount of palladium oxide. Thus, we chose 0.7 V as the optimum potential for generating a sufficiently large amount of manganese oxide for detection without causing problems with peak height measurement because of the interfering palladium oxide reduction wave.

We evaluated the effect of preconcentration time on sensitivity (Figure 5c) to find the minimum time for adequate sensitivity (i.e., substantial depletion of metal ion from the sample). We observed the usual increase in Mn peak amplitude with deposition time as more Mn from the sample was deposited on the WE. The coefficients of variation of the stripping peak for 5 and 10 min were both 11%, illustrating that 5 and 10 min could generate reproducible voltammograms. This high degree of reproducibility illustrates an excellent performance for a disposable sensor. But at 15 min it dramatically increased to ~39%, suggesting a major change in the condition of the WE. We found that the thin Pd film was not sufficiently thick to protect the underlying Cu layer for such a long deposition time during which some Pd was being oxidized. We observed gradual peeling at the edges of the Pd film on both the WE and the AE which exposed Cu, making it available for oxidation at the deposition potential and disrupting Mn preconcentration. Under agitation, the Pd film was easily removed, leaving only the 20 nm of Ti seed layer to


dx.doi.org/10.1021/ac502882s | Anal. Chem. 2014, 86, 12070–12077

sustain the current. This created a sudden increase in resistance that was accompanied by disintegration of the WE, and the sensor could no longer perform the experiment and had to be discarded. Consequently, we chose 10 min for the preconcentration time to maximize the stripping peak for Mn while consistently avoiding this problem with WE durability. A shorter preconcentration time may be possible in the future if agitation of the sample is improved, for example, by using an acoustic transducer.[49]

Optimum waveform parameters for stripping by square wave (SW) voltammetry were found to be the default Osteryoung settings[45] of 25 mV amplitude, 70 ms period, and 4 mV increment. Varying the waveform parameters sometimes increased the peak height, but always tended to distort the voltammograms, broaden the peaks, or even create huge peaks in the background, making it challenging to accurately quantify the Mn peak current. Therefore, we used the default values for Osteryoung square wave voltammetry.

**Calibration in Borate Buffer.** Following optimization of experimental and stripping waveform parameters, a calibration curve was constructed by performing CSV in 100 $\mu$L of borate buffer (0.1 M, pH 9.0) with 25−600 ppb (455 nM to 10.9 $\mu$M) of Mn spiked, as shown in Figure 6. This range brackets the

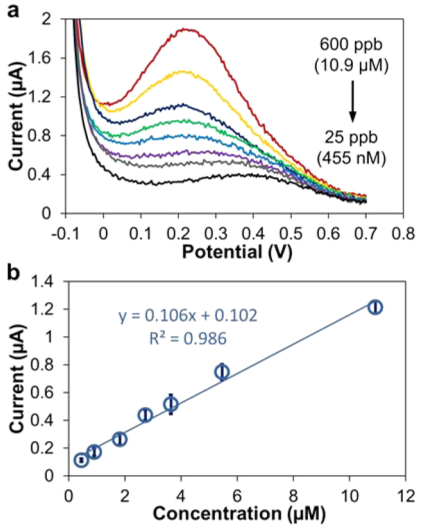


**Figure 6.** SWCSV determination of Mn in pH 9.0, 0.1 M borate buffer for the 25−600 ppb (455 nM to 10.9 $\mu$M) range: (a) stripping voltammograms of Mn; (b) calibration curve plotted after baseline subtraction. Sample volume, 100 $\mu$L; preconcentration potential, 0.7 V; preconcentration time, 600 s; period, 70 ms; increment, 4 mV; amplitude, 25 mV.

range of Mn in environmental samples, while illustrating that the LOD of the sensor allows for multifold dilution, if necessary. For most concentrations, we repeated experiments three times ($n$ = 3) using a new disposable sensor each time to obtain the standard deviation $\sigma$ ($n$ = 7 was used for the lowest Mn concentration). Representative stripping voltammograms over the entire 500 nM to 10.9 $\mu$M concentration range are shown in Figure 6a.

The Mn peak occurred at 212−216 mV in Mn concentrations from 150−600 ppb, and shifted to ∼226 mV in 50−100 ppb Mn levels, then shifted further to ∼270 mV when Mn concentration dropped to 25 ppb. Since a minor peak at 381 ± 16 mV in the borate buffer background voltammogram (black) could be observed, it is believed to be due to palladium oxide only. Thus, we attribute the positive shift of peak potential that accompanies decreasing of Mn levels to the interference of a minute amount of palladium oxide formed on top of the Pd electrode, which tends to compete with the formation of manganese oxide for WE surface area. This has been a common issue with solid electrodes. As we gradually increased Mn levels, the reduction of manganese oxide surpassed the reduction of palladium oxide and then Mn stripping became predominant and the peak shifted to ∼220 mV. We have previously observed similar concentration-related peak migration in ASV of Zn using a Bi WE,[33] which was also caused by modification to the electrode surface and could cause resolution issues in the lower concentration range of the analyte.

After we obtained the voltammograms, a baseline subtraction method was used to remove the interference of the minor wave present in the background voltammograms to ensure the accuracy of readouts of Mn peak amplitude. This approach involves first creating a virtual average curve of several actual background curves ($n$ = 4) generated in pH 9.0, 0.1 M borate buffer using a new sensor each time and then subtracting this virtual curve from each original voltammogram. The resulting voltammograms then exhibited the reduction peak of manganese oxide only. After baseline subtraction, clean Mn peak amplitudes were measured to plot the calibration curve and to calculate detection limit.

The resulting calibration curve (Figure 6b) exhibited a strong linear relationship between peak current of Mn stripping and Mn concentration. The correlation equation was $I$ ($\mu$A) = $(0.106(\pm 0.006))([\text{Mn}\ (\mu\text{M})]) + 0.10_2(\pm 0.02_8)$ ($R^2$ = 0.986 for 7 data points). The sensor exhibited good sensitivity 0.106 $\mu$A/$\mu$M ($5.57_5$ $\mu$A/$\mu$M/cm$^2$ when normalized to WE area). The detection limit was calculated to be LOD = 334 nM (18.3 ppb) based on 3$\sigma$/slope ($n$ = 7). Measurements of Mn using bulk electrodes reported by Banks et al.[4] showed a 740 nM LOD using ASV on a boron-doped diamond electrode, while Yue et al.[5] reported 120 and 93 nM LODs for ASV and CSV using a metal catalyst free CNT electrode. Compared with these bulk electrodes, our Pd microelectrode is able to provide competitive performance and yet more convenient measurements.

**Determination of Water Manganese.** To demonstrate performance of our sensor in environmental samples, we chose samples of water from the Ohio River and a pond in Burnet Woods, OH as representative natural water samples. We first tested pond water and spiked it with Mn (see the Supporting Information), since water from this pond was previously examined by AAS and CSV and showed no detectable Mn.[5] We spiked 73.6 ppb of Mn into the sample, measured $71._3 \pm 8._7$ ppb of Mn using the standard addition method. This demonstrates accuracy of 97% with 17% precision ($n$ = 3). This experiment demonstrates the capability of our Pd WE to accurately determine concentrations of Mn in a natural water sample.

On the basis of the performance in a spiked water sample, we used our sensor to determine unknown Mn concentration in a river water sample. We also diluted the sample with pH 9.0, 0.2 M borate buffer by a factor of 2×. The standard addition method was again applied, using 50, 100, and 200 ppb of additional Mn. The voltammograms in Figure 7a illustrate the peak potentials of different concentrations of Mn to be 296, 196, 156, and 184 mV, respectively, showing the RE was influenced by the water sample matrix as well. They follow the migration profile related to Mn levels as discussed in previous


dx.doi.org/10.1021/ac502882s | Anal. Chem. 2014, 86, 12070−12077

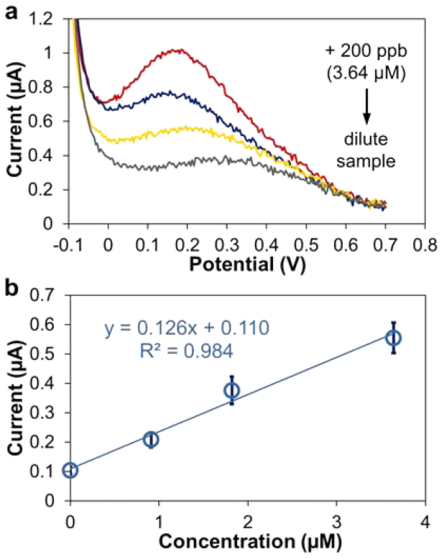


**Figure 7.** Determination of Mn in spiked Ohio River water using SWCSV and the standard addition method. Samples were diluted 2× with 0.2 M borate buffer pH 9.0 and for standard addition of 50−200 ppb Mn. (a) Voltammograms of spiked sample and four additions of Mn standards and (b) standard addition curve after baseline subtraction.

sections. Since the amplitude of the Mn peak of the unspiked sample remains slightly obscure which suggested the need for baseline subtraction, we applied the same treatment to these voltammograms. According to Figure 7b, the correlation equation is $I$ ($\mu$A) = $(0.12_6(\pm 0.01_1))([\text{Mn}\ (\mu\text{M})])$ + $0.11_0(\pm 0.02_3)$ ($R^2$ = 0.984 for 4 data points). We calculated the Mn concentration using the equation above while considering the dilution factor. The Mn concentration in Ohio River was determined as $1.7_4 \pm 0.4_9$ $\mu$M ($95._4 \pm 27._0$ ppb), which is in the range of Mn present in surface waters (typically 1 ppb to 1 ppm[46−48]).

In environmental samples, the potentially interfering species present in the sample can be broadly divided into nonelectroactive and electroactive components. The nonelectroactive components do not participate in the preconcentration and stripping of Mn, and thus do not impact sensor performance. The electroactive metal components, such as $Fe^{2+}$, $Fe^{3+}$, $Cd^{2+}$, $Cu^{2+}$, $Ni^{2+}$, $Zn^{2+}$, $Pb^{2+}$, $As^{3+}$, $Se^{4+}$, can exist in any sample matrix. However, most of these species have very specific reduction/oxidation potentials and are not likely to interfere with Mn due to difference in the stripping potential. Also, previous work by Saterlay et al.[31] indicated that $Zn^{2+}$, $Cu^{2+}$, $Pb^{2+}$, and $Fe^{3+}$ have no measurable effect for Mn determination. Recent work by Banks et al.[4] and Locatelli and Torsi[21] independently confirmed that the only considerable interference in such measurements could be due to $Fe^{2+}$, and that CSV is highly selective toward Mn. Thus, CSV is ideally suited for complex environmental samples such as those reported herein.

## CONCLUSIONS

We demonstrated a palladium-based electrochemical sensor for CSV and demonstrated the determination of Mn in buffer and environmental water samples. Compared with ASV, CSV is a viable alternative for detecting metals whose reduction potentials are too negative for the potential window of common WEs in ASV. This work also showcases the flexibility of our copper-based sensor platform, which can be easily modified by simple coating of the WE surface. To our knowledge, this is also the first demonstration of Mn determination by CSV on a microscale sensor.

Several features make this sensor ideally suited for POC applications. First, Pd is a relatively low-cost electrode material compared to Au or Pt. Though Pd is not a commonly used material for electroanalytical systems, it provides stable potential as AE and sufficient potential window for CSV of Mn as WE. We also demonstrated that the sensor with a Cu/$CuCl_2$ RE was sufficiently stable for CSV with a preconcentration time as long as 600 s. Thus, the sensors are qualified to be low-cost disposable sensors for POC instruments. Second, the microfabrication procedure of our palladium-based sensor is relatively simple. Microfabrication offers the potential for mass production, which can further reduce the cost of the sensor. Simple fabrication also helps to reduce the device-to-device variation, leading to relatively low 11% variability. This advantage is crucial for POC applications where disposable sensors are used, as it becomes possible to minimize errors introduced through sensor manufacturing.

Finally, the sensor offers competitive performance for electrochemical determination of Mn. By optimizing experimental parameters, the sensor exhibits LOD = 334 nM (18.3 ppb), good sensitivity of 0.106 $\mu$A/$\mu$M ($5.57_5$ $\mu$A/$\mu$M/cm$^2$ normalized to WE area), and good linearity in the 455 nM to 10.9 $\mu$M range. This is a significant improvement in performance compared with our previous work. In experiments with water samples, good quality peaks were observed that can be used to quantify the concentration of Mn using the method of standard additions. Ultimately, while our miniaturized palladium-based voltammetric sensors are unable to match the precision and limits of detection of modern spectroscopic and mass spectrometry techniques, the measurements that they are able to do are in the relevant range and use low-cost materials with simple fabrication, which is more favorable for disposable sensors.

## ASSOCIATED CONTENT

### Supporting Information

Supporting information as noted in the text, which includes discussion of the Pd WE potential window and Mn determination in spiked pond water samples. This material is available free of charge via the Internet at http://pubs.acs.org.

## AUTHOR INFORMATION

### Corresponding Author

*Phone: 513-556-2347. Fax: 513-556-7326. E-mail: ian.papautsky@uc.edu.

### Notes

The authors declare no competing financial interest.

## ACKNOWLEDGMENTS

This work was supported by funds provided by the National Institutes of Health (NIH) awards R21ES019255 and R01ES022933.

## REFERENCES

(1) Gadd, G. M.; Griffiths, A. J. *Microb. Ecol.* **1978**, *4*, 303−317.
(2) Keen, C. L.; Ensunsa, J. L.; Clegg, M. S. In *Metal Ions in Biological Systems: Volume 37: Manganese and Its Role in Biological Processes*; Sigel, A., Sigel, H., Eds.; Marcel Dekker, Inc.: New York, 2000; pp 89−121.
(3) Witholt, R.; Gwiazda, R.; Smith, D. *Neurotoxicol. Teratol.* **2000**, *22*, 851−861.

(4) Banks, C. E.; Kruusma, J.; Moore, R. R.; Tomčík, P.; Peters, J.; Davis, J.; Komorsky-Lovrić, Š; Compton, R. G. *Talanta* **2005**, *65*, 423−429.
(5) Yue, W.; Bange, A.; Riehl, B. L.; Riehl, B. D.; Johnson, J. M.; Papautsky, I.; Heineman, W. R. *Electroanalysis* **2012**, *24*, 1909−1914.
(6) Claus Henn, B.; Ettinger, A. S.; Schwartz, J.; Tellez-Rojo, M. M.; Lamadrid-Figueroa, H.; Hernandez-Avila, M.; Schnaas, L.; Amarasiriwardena, C.; Bellinger, D. C.; Hu, H.; Wright, R. O. *Epidemiology* **2010**, *21*, 433−439.
(7) Rugless, F.; Bhattacharya, A.; Succop, P.; Dietrich, K. N.; Cox, C.; Alden, J.; Kuhnell, P.; Barnas, M.; Wright, R.; Parsons, P. J.; Praamsma, M. L.; Palmer, C. D.; Beidler, C.; Wittberg, R.; Haynes, E. N. *Neurotoxicol. Teratol.* **2014**, *41*, 71−79.
(8) Standridge, J. S.; Bhattacharya, A.; Succop, P.; Cox, C.; Haynes, E. *J. Occup. Environ. Med.* **2008**, *50*, 1421−1429.
(9) Haynes, E. N.; Heckel, P.; Ryan, P.; Roda, S.; Leung, Y.-K.; Sebastian, K.; Succop, P. *Neurotoxicology* **2010**, *31*, 468−474.
(10) Haynes, E. N.; Ryan, P.; Chen, A.; Brown, D.; Roda, S.; Kuhnell, P.; Wittberg, D.; Terrell, M.; Reponen, T. *Sci. Total Environ.* **2012**, *427−428*, 19−25.
(11) Hue, N. V.; Vega, S.; Silva, J. A. *Soil Sci. Soc. Am. J.* **2001**, *65*, 153−160.
(12) Davis, J. M.; Jarabek, A. M.; Mage, D. T.; Graham, J. A. *Risk Anal.* **1998**, *18*, 57−70.
(13) Zayed, J.; Guessous, A.; Lambert, J.; Carrier, G.; Philippe, S. *Sci. Total Environ.* **2003**, *312*, 147−154.
(14) Morrow, H. *Ind. Chem. Libr.* **2001**, *10*, 1−34.
(15) Williams, M.; Todd, G. D.; Roney, N.; Crawford, J.; Coles, C.; McClure, P. R.; Garey, J. D.; Zaccaria, K.; Citra, M. *Toxicological Profile for Manganese*; Agency for Toxic Substances and Disease Registry: Atlanta, GA, 2012.
(16) Woolf, A.; Wright, R.; Amarasiriwardena, C.; Bellinger, D. *Environ. Health Perspect.* **2002**, *110*, 613−616.
(17) Strobel, H., Heineman, W., Eds. *Chemical Instrumentation: A Systematic Approach*, 3rd ed.; Wiley: New York, 1989; p 1137.
(18) Kissinger, P. T.; Heineman, W. R. *Laboratory Techniques in Electroanalytical Chemistry*, 2nd ed.; Marcel Dekker, Inc.: New York, 1996.
(19) Wang, J. *Analytical Electrochemistry*, 3rd ed.; John Wiley & Sons, Inc.: Hoboken, NJ, 2006.
(20) Jothimuthu, P.; Wilson, R. A.; Herren, J.; Haynes, E. N.; Heineman, W. R.; Papautsky, I. *Biomed. Microdevices* **2011**, *13*, 695−703.
(21) Locatelli, C.; Torsi, G. *J. Electroanal. Chem.* **2001**, *509*, 80−89.
(22) Hrabankova, E.; Doležal, J.; Mašin, V. *J. Electroanal. Chem. Interfacial Electrochem.* **1969**, *22*, 195−201.
(23) Ishiyama, T.; Tanaka, T. *Tetsu to Hagane (Journal of the Iron and Steel Institute of Japan)* **1996**, *82*, 923−928.
(24) Ishiyama, T. *Bunseki Kagaku* **1997**, *46*, 847−848.
(25) Brett, C. M. A.; Neto, M. M. P. M. *J. Electroanal. Chem. Interfacial Electrochem.* **1989**, *258*, 345−355.
(26) Roitz, J. S.; Bruland, K. *Anal. Chim. Acta* **1997**, *344*, 175−180.
(27) Di, J.; Zhang, F. *Talanta* **2003**, *60*, 31−36.
(28) Filipe, O.; Brett, C. *Talanta* **2003**, *61*, 643−650.
(29) Labuda, J.; Vanícková, M.; Beinrohr, E. *Microchim. Acta* **1989**, *97*, 113−120.
(30) Justino, C. I. L.; Rocha-Santos, T. A. P.; Duarte, A. C. *TrAC, Trends Anal. Chem.* **2013**, *45*, 24−36.
(31) Saterlay, A. J.; Foord, J. S.; Compton, R. G. *Analyst* **1999**, *124*, 1791−1796.
(32) Pei, X.; Kang, W.; Yue, W.; Bange, A.; Heineman, W. R.; Papautsky, I. *Anal. Chem.* **2014**, *86*, 4893−4900.
(33) Kang, W.; Pei, X.; Yue, W.; Bange, A.; Heineman, W. R.; Papautsky, I. *Electroanalysis* **2013**, *25*, 2586−2594.
(34) Lee, J. K.; Adams, R. N.; Bricker, C. E. *Anal. Chim. Acta* **1957**, *17*, 321−328.
(35) Souto, R. M.; Rodríguez, J. L.; Fernández-Mérida, L.; Pastor, E. *J. Electroanal. Chem.* **2000**, *494*, 127−135.
(36) Jeong, M.; Pyun, C. H.; Yeo, I. *J. Electrochem. Soc.* **1993**, *140*, 1986−1989.
(37) Grdeń, M.; Łukaszewski, M.; Jerkiewicz, G.; Czerwiński, A. *Electrochim. Acta* **2008**, *53*, 7583−7598.
(38) Khudaish, E. A.; Farsi, A. A. A. *Talanta* **2010**, *80*, 1919−1925.
(39) Suzuki, H.; Shiroishi, H.; Sasaki, S.; Karube, I. *Anal. Chem.* **1999**, *71*, 5069−5075.
(40) Matsumoto, T.; Ohashi, A.; Ito, N. *Anal. Chim. Acta* **2002**, *462*, 253−259.
(41) Kinoshita, E.; Ingman, F.; Edwall, G.; Glab, S. *Electrochim. Acta* **1986**, *31*, 29−38.
(42) Abys, J. A. In *Modern Electroplating*; Schlesinger, M., Paunovic, M., Eds.; John Wiley & Sons: Hoboken, NJ, 2010; pp 327−368.
(43) Raub, C. J. *Platinum Met. Rev.* **1982**, *26*, 158−166.
(44) Rosamilia, J.; Abys, J.; Miller, B. *Electrochim. Acta* **1991**, *36*, 1203−1208.
(45) Osteryoung, J. G.; Osteryoung, R. A. *Anal. Chem.* **1985**, *57*, 101A−110A.
(46) Colombini, M.; Fuoco, R. *Talanta* **1983**, *30*, 901−905.
(47) Youger, J. D.; Mitsch, W. J. *Ohio J. Sci.* **1989**, *89*, 172−175.
(48) Lesven, L.; Skogvold, S. M.; Mikkelsen, Ø.; Billon, G. *Electroanalysis* **2009**, *21*, 274−279.
(49) Patel, M. V.; Nanayakkara, I. A.; Simon, M. G.; Lee, A. P. *Lab Chip* **2014**, *14*, 3860−3872.